

THE PHYSICS AND COSMOLOGY OF TEV BLAZARS IN A NUTSHELL

C. PFROMMER¹, A. E. BRODERICK², P. CHANG³, E. PUCHWEIN¹, V. SPRINGEL^{1,4}

¹ *Heidelberg Institute for Theoretical Studies, Schloss-Wolfsbrunnengasse 35, 69118 Heidelberg, Germany*

² *Perimeter Institute for Theoretical Physics, 31 Caroline Street North, Waterloo, ON, N2L 2Y5, Canada; Department of Physics and Astronomy, University of Waterloo, 200 University Avenue West, Waterloo, ON, N2L 3G1, Canada*

³ *Department of Physics, University of Wisconsin-Milwaukee, 1900 E. Kenwood Boulevard, Milwaukee, WI 53211, USA*

⁴ *Zentrum für Astronomie der Universität Heidelberg, Astronomisches Recheninstitut, Mönchhofstr. 12-14, 69120 Heidelberg, Germany*

The extragalactic gamma-ray sky at TeV energies is dominated by blazars, a subclass of accreting super-massive black holes with powerful relativistic outflows directed at us. Only constituting a small fraction of the total power output of black holes, blazars were thought to have a minor impact on the universe at best. As we argue here, the opposite is true and the gamma-ray emission from TeV blazars can be thermalized via beam-plasma instabilities on cosmological scales with order unity efficiency, resulting in a potentially dramatic heating of the low-density intergalactic medium. Here, we review this novel heating mechanism and explore the consequences for the formation of structure in the universe. In particular, we show how it produces an inverted temperature-density relation of the intergalactic medium that is in agreement with observations of the Lyman- α forest. This suggests that *blazar heating* can potentially explain the paucity of dwarf galaxies in galactic halos and voids, and the bimodality of galaxy clusters. This also transforms our understanding of the evolution of blazars, their contribution to the extra-galactic gamma-ray background, and how their individual spectra can be used in constraining intergalactic magnetic fields.

1 Introduction

The extragalactic gamma-ray sky is dominated by “blazars”. These are a subclass of super-massive black holes, situated at the center of every galaxy, which drive powerful relativistic jets and electromagnetic radiation out to cosmological distances. An important subset of blazars exhibit hard power-law spectra that extend to TeV photon energies (high-energy-peaked BL Lacs). The Universe is opaque to the emitted TeV gamma rays because they annihilate and pair produce on the extragalactic background light which is emitted by galaxies and quasars through the history of the universe. The mean free path for this reaction is $\lambda_{\gamma\gamma} \sim (700 \dots 35) (E/\text{TeV})^{-1}$ Mpc for redshifts $z = 0 \dots 1$, respectively, and is approximately constant at $\lambda_{\gamma\gamma} \sim 35 (E/\text{TeV})^{-1}$ Mpc for higher redshifts. The resulting ultra-relativistic pairs of electrons and positrons are commonly assumed to lose energy primarily through inverse Compton scattering with photons of the cosmic microwave background, cascading the original TeV emission a factor of $\sim 10^3$ down to GeV energies.

However, there are two serious problems with this picture: the expected cascaded GeV emission is not seen in the individual spectra of those blazars (Neronov & Vovk 2010) and the emission of all unresolved blazars would overproduce the observed extragalactic gamma-ray background (EGRB) at GeV energies *if* these objects share a similar cosmological evolution as

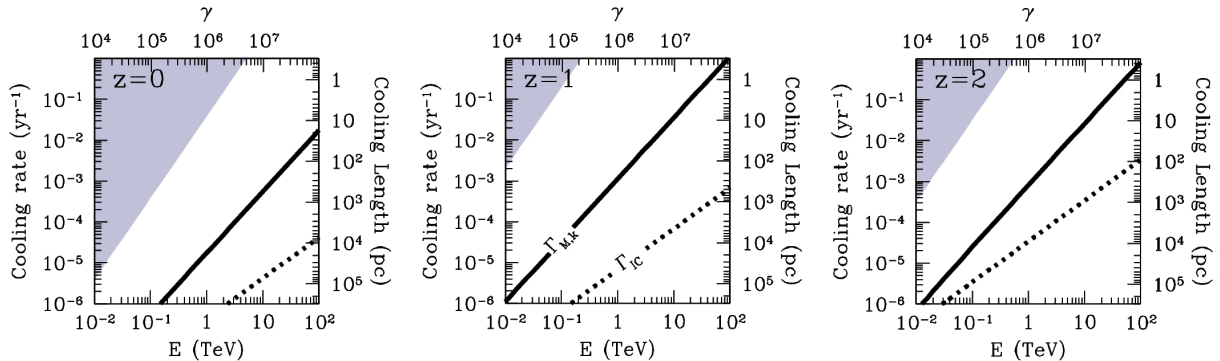


Figure 1: Initial pair beam cooling rates due to the kinetic oblique instability (thick solid) and inverse Compton scattering (dotted) as a function of gamma-ray energy (E) at a number of redshifts (z). In all cases, we consider a mean-density region, and the isotropic-equivalent luminosity of the source at energy E , EL_E , is 10^{45} erg s $^{-1}$, similar to the brightest TeV blazars seen from Earth. We list the initial pair Lorentz factor, γ , and cooling lengthscales along the top and right axes, respectively (from Broderick *et al.* 2012).

the underlying black hole or parent galaxy population (Venters 2010). As a putative solution to the first problem, comparably large magnetic fields have been hypothesized which would deflect the pairs out of our line-of-sight to these blazars (Neronov & Vovk 2010), diluting the point-source flux into a lower surface brightness “pair halo”. However, magnetic deflection of pairs (and hence their inverse Compton emission) out of our line-of-sight is on average balanced by deflecting other pairs into our line-of-sight, so that the resulting isotropic EGRB remains invariant. This represents a substantial problem to unifying the hard gamma-ray blazar population with that of other active galactic nuclei (AGN), is at odds with the underlying physical picture of accreting black hole systems, and suggests an unlikely conspiracy between accretion physics and the formation of structure.

2 Beam-plasma instabilities

Recently, we have shown that there is an even more efficient mechanism that competes with this cascading process. Plasma instabilities driven by the highly anisotropic nature of the ultra-relativistic pair distribution provide a plausible way to dissipate the kinetic energy of the TeV pairs locally, heating the intergalactic medium (Broderick *et al.* 2012). We can understand the two-stream instability intuitively by considering a longitudinal wave-like perturbation of the charge of the background plasma along the beam direction (i.e., a Langmuir wave). The initially homogeneous beam electrons feel repulsive (attractive) forces by the potential minima (maxima) of the electrostatic wave in the background plasma. As a result, electrons (positrons) attain their lowest velocity in the potential minima (maxima), which causes them to bunch up. Hence, the bunching within the beam is simply an excitation of a beam Langmuir wave that couples in phase with the background perturbation. This enhances the background potential and implies stronger forces on the beam pairs. This positive feedback loop causes exponential wave-growth, i.e. the onset of an instability. In practice, oscillatory modes that propagate in an oblique direction to the beam grow substantially faster than the two-stream instability just discussed. The reason is that electric fields can more easily deflect ultra-relativistic particles than change their parallel velocities (see Broderick *et al.* 2012, for details).

Unstable electromagnetic waves grow fastest when the velocity dispersions are smallest across their wave fronts. As these velocity dispersions get larger and larger, i.e., for increasing temperature, the growth rate of the unstable oblique mode moves into the finite temperature or kinetic regime, where the exponential growth rate is reduced due to the effects of phase mixing and decoherence. In Fig. 1, we show the pair beam cooling rates due to the kinetic oblique instability in the linear regime, $\Gamma_{M,k}$ (Bret *et al.* 2010a) for a beam density that obeys the

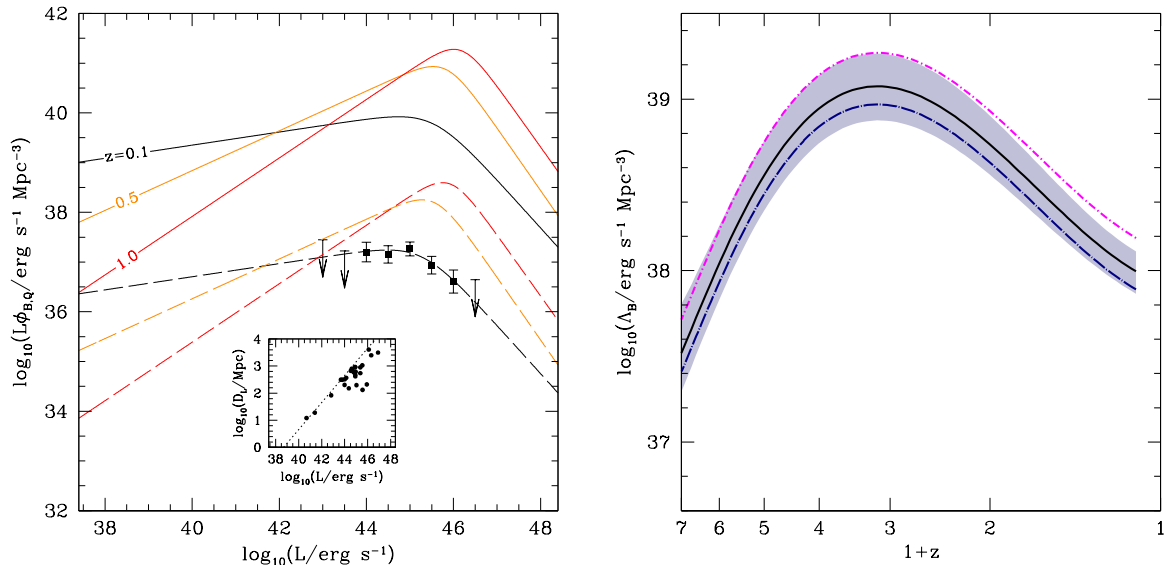


Figure 2: *Left.* Comparison between the luminosity-weighted quasar and TeV-blazar luminosity functions ($L\phi_Q(z, L)$ and $L\phi_B(z, L)$, respectively). The solid lines show the absolute $L\phi_Q$ (in comoving Mpc), while the dashed lines show $L\phi_Q$ rescaled in magnitude by 2.1×10^{-3} and shifted to lower luminosities by a factor of 0.55. Different redshifts are color coded as indicated in the figure. The points and upper-limits show ϕ_B of all high- and intermediate-energy-peaked blazars with good spectral measurements. Presented in the inset is the TeV source luminosity distance as a function of source luminosity for all of the blazars with redshift estimates (including limits). The dotted line shows the distance-dependence of the flux limit we employ in the completeness correction (from Broderick *et al.* 2012). *Right.* Comoving blazar luminosity density $\Lambda_B(z) = \int_{L_{\text{min}}}^{\infty} dL \phi_B(z, L)$ as a function of redshift. The shaded region represents the $1\text{-}\sigma$ uncertainty that results from a combination of the uncertainty in the number of bright blazars that contribute to the local heating and in the uncertainties in the quasar luminosity density (Hopkins *et al.* 2007) to which we normalize (from Chang *et al.* 2012).

steady-state Boltzmann equation, i.e., we account for production and various loss processes of the pairs. Most importantly, we find that $\Gamma_{M,k}$ dominates over the inverse Compton cooling rate Γ_{IC} by more than an order of magnitude for the parameters of luminous TeV blazars.

Analytical quasi-linear calculations of the cold regime (Schlickeiser *et al.* 2012) and numerical work of the oblique instability in the kinetic regime (Bret *et al.* 2010b) with smaller density contrasts than considered here suggest that the dominance of the oblique instability carries over in the regime of non-linear saturation, although there is currently a debate about the role of induced scattering by thermal ions on this non-linear saturation (Miniati & Elyiv 2013, Schlickeiser *et al.* 2013, Chang *et al.* in prep.). In the following, we assume that a large fraction of the free kinetic energy of the pairs is transferred to the electromagnetic modes in the background plasma, which should eventually be dissipated, heating the intergalactic medium (IGM).

3 Implications for the blazar luminosity function and the gamma-ray sky

To assess implications for the gamma-ray sky and the thermal evolution of the IGM, we construct a blazar luminosity function (BLF). In Broderick *et al.* (2012), we collect the luminosity of all 23 TeV blazars with good spectral measurements and account for selection effects (sky coverage, duty cycle, galactic occultation, TeV flux limit). The resulting BLF is shown in Fig. 2. Most notably, the TeV blazar luminosity density is a scaled version of that of quasars. This implies that quasars and TeV blazars appear to be regulated by the same mechanism and are contemporaneous elements of a single AGN population, i.e., the TeV-blazar activity does not lag quasar activity. Hence we adopt the plausible assumption that both distributions trace each other for all redshifts and work out the implications of this assertion.

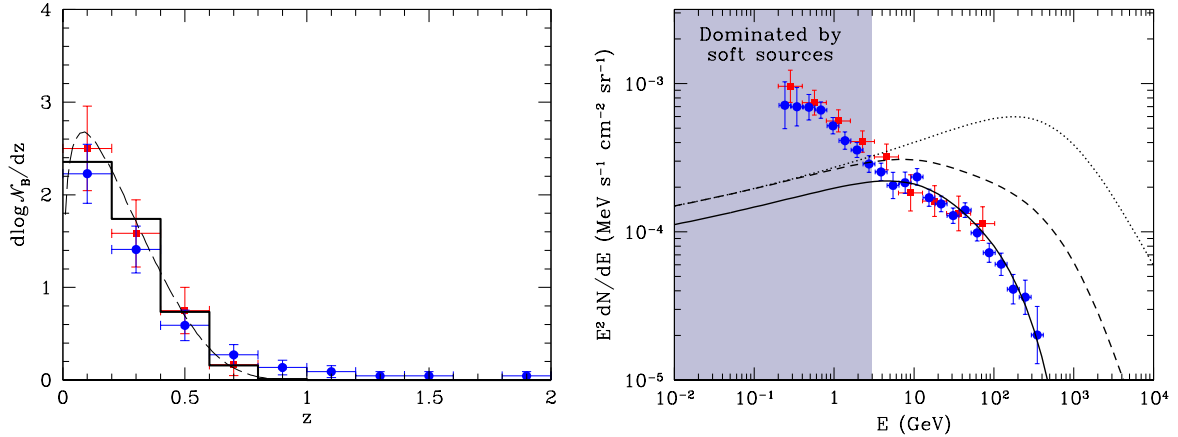


Figure 3: *Left.* Nearby redshift distribution of the hard gamma-ray blazars above the *Fermi* flux limit, both in continuous form (dashed) and binned with $\Delta z = 0.2$ (continuous). For comparison the redshift distribution of the *Fermi* hard gamma-ray blazars in the 1LAC (red squares) and 2LAC (blue circles) are also shown. For these, the vertical error bars denote Poisson errors. *Right.* *Fermi* EGRB anticipated by the hard gamma-ray blazars. The dotted, dashed, and solid lines correspond to the unabsorbed spectrum, spectrum corrected for absorption on the extragalactic background light, and spectrum additionally corrected for resolved point sources (assuming all hard gamma-ray blazars with $z \lesssim 0.29$ are resolved). These are compared with the measured *Fermi* EGRB reported in Abdo *et al.* (2010, red squares) and Ackermann *et al.* (2012, blue circles). Note that below ~ 3 GeV the EGRB is dominated by soft sources (from Broderick *et al.* 2013).

To quantify the impact on the gamma-ray sky, we need to expand the BLF to include the intrinsic energy spectra, dN/dE , of blazars and adopt a typical broken power-law spectrum

$$\frac{dN}{dE} = f \hat{F}_E = f \left[\left(\frac{E}{E_b} \right)^{\Gamma_l} + \left(\frac{E}{E_b} \right)^{\Gamma_h} \right]^{-1}, \quad (1)$$

where $E_b \simeq 1$ TeV is the break energy, $\Gamma_h \simeq 3$ is the high-energy spectral index, and the intrinsic low-energy slope Γ_l is softened with increasing propagation length due to the higher probability of high-energy photons to annihilate on the extragalactic background light. This yields a steeper (larger) observed Γ_F , which we draw from the distribution of local blazars as observed by the *Fermi* gamma-ray telescope (that are not affected by spectral softening due to pair production effects). We arrive at the BLF, $d^4\mathcal{N}/(d \log L_{\text{TeV}} dz dE d\Gamma_l)$, i.e., the distribution of blazars with TeV luminosity L_{TeV} , redshift z , gamma-ray energy E , and Γ_l .

Different projections of this BLF onto its independent variables allow comparison to *Fermi* data. Integrating this distribution over L_{TeV} , E and Γ_l and adopting integration limits that account for the *Fermi* flux limit S_{min} yields the redshift distribution of *Fermi* blazars (left panel of Fig. 3). Interestingly, an evolving (increasing) blazar population is consistent with the observed declining number evolution of blazars due to the *Fermi* flux limit and the low intrinsic luminosity of the hard blazars. Masking these resolved blazars and integrating the blazar distribution over L_{TeV} , z , and Γ_l yields the contribution of blazars to the *isotropic* EGRB (right panel of Fig. 3). This demonstrates that an evolving population of hard blazars matches the latest data of the EGRB by the *Fermi* Collaboration at energies $\gtrsim 3$ GeV extremely well. Moreover, the modeled $\log \mathcal{N}$ - $\log S$ distribution and the *anisotropic* EGRB, which mainly probes nearby objects below the detectability limit, provide an excellent match to the *Fermi* data (Broderick *et al.* 2013). Hence, this naturally solves the two mysteries introduced in Sect. 1 in a *unified model of blazars and their underlying black hole population without the need to invoke large magnetic fields*. Critical to this success is the absence of inverse Compton cascades that would otherwise redistribute energy between the unabsorbed and the absorbed spectrum into the energy range around 10 GeV, thus vastly overproducing the tight limits provided by *Fermi*.

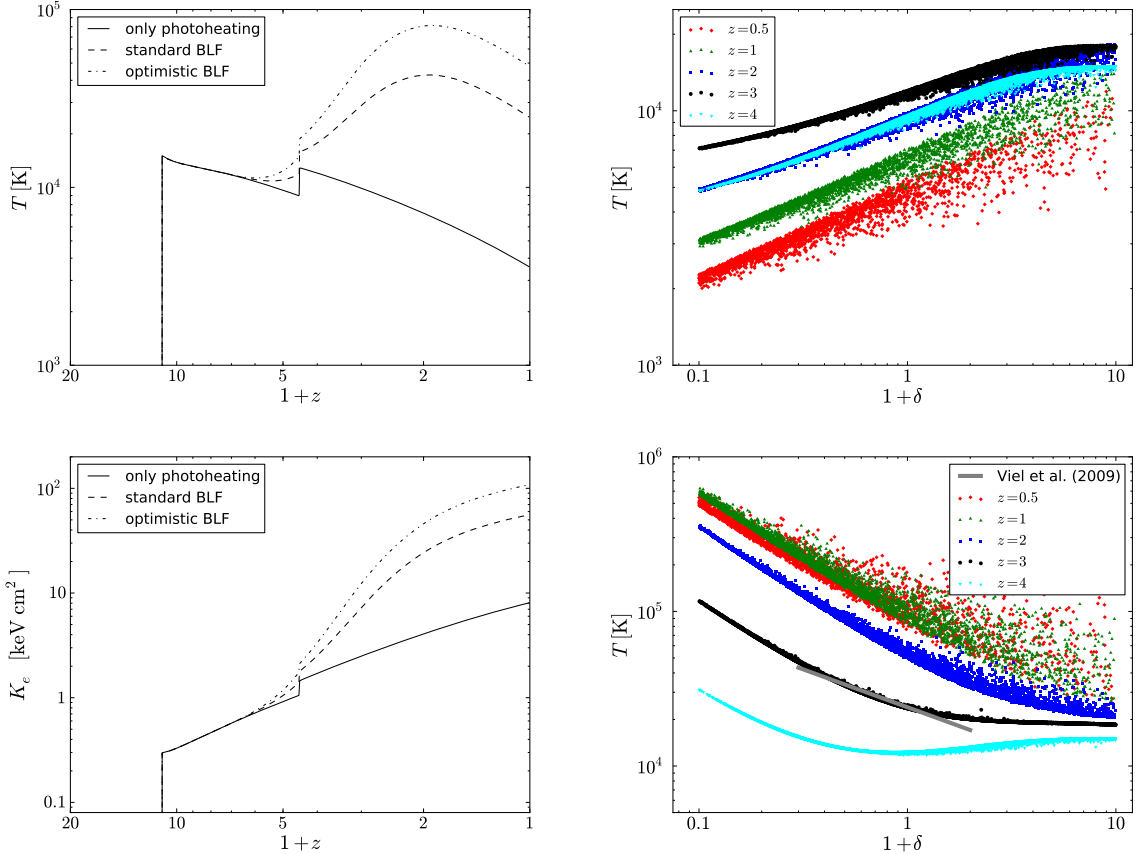


Figure 4: Thermal history (*top left*) and entropy history (*bottom left*) of a patch of mean density ($\delta = 0$) of the IGM. The solid curves are for pure photoheating with sudden reionization histories for H and He II at $z_{\text{reion}} = 10$ and $z_{\text{He II}} = 3.5$. The dashed (dash-dotted) lines show the evolution for the standard (optimistic) blazar heating model that employs the blazar luminosity density, i.e., using the redshift evolution of the quasar luminosity density and are normalized to the local heating rate, which is subject to an uncertain incompleteness correction factor (from Pfrommer *et al.* 2012). Temperature-density relation without blazar heating (*top right*) and for the optimistic blazar heating model (*bottom right*) at a number of redshifts (from Chang *et al.* 2012). The grey line is the best-fit model derived from Lyman- α data (Viel *et al.* 2004).

4 Rewriting the thermal history of the IGM and the Lyman- α forest

We find that for our BLF, every region in the universe is heated by at least one TeV blazar back to $z \sim 5$, providing a novel heating mechanism of the gas at mean density that is ten times larger at the present time than what has been previously considered (Chang *et al.* 2012). This can be interpreted as a gradually rising (and density dependent) entropy enhancement after $z = 3$ (left panels of Fig. 4). Unlike photoheating, the blazar heating rate per unit volume does not depend on density since (1) the distributions of TeV blazars and the extragalactic background light are uniform on the cosmological scales of the mean free path of pair production, $\lambda_{\gamma\gamma}$, and (2) it is nearly independent of the IGM density. Hence this particular heating process deposits more energy per baryon in low-density regions and naturally produces an inverted temperature-density relation in voids that reaches asymptotically $T \propto 1/\rho$ (right panels of Fig. 4). This unique property in combination with the recent and continuous nature of blazar heating is needed to solve many problems present in previous calculations of Lyman- α forest spectra.

Detailed cosmological simulations that include blazar heating show superb agreement with all statistics used to characterize Lyman- α forest spectra (Puchwein *et al.* 2012). In particular, our simulations with blazar heating simultaneously reproduce the observed effective optical depth and temperature as a function of redshift, the observed probability distribution functions

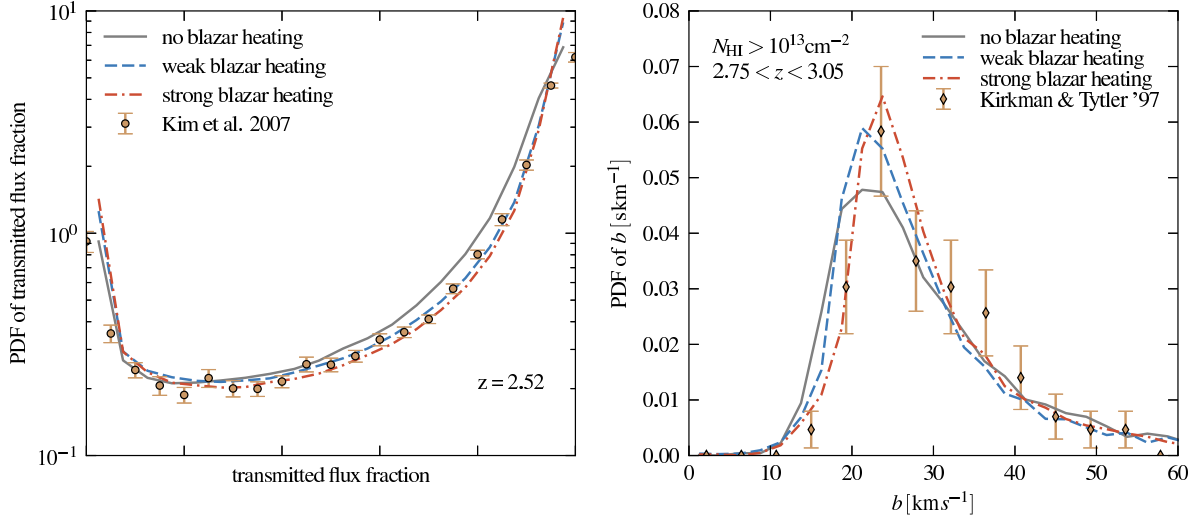


Figure 5: Comparing the Lyman- α forest in hydrodynamical cosmological simulations with and without blazar heating. *Left.* Probability distribution functions of the transmitted flux fraction for simulations with and without blazar heating for two different normalisations of the blazar heating rate are compared to observational constraints from Kim *et al.* 2007. *Right.* The normalised distribution function of Lyman- α line widths, b , for simulations with and without blazar heating at redshift $z = 3$ are compared to observational constraints by Kirkman *et al.* (1997). Both panels show simulation results for a UV background that was *matched* to the observed mean transmission (from Puchwein *et al.* 2012).

of the transmitted flux (Fig. 5), and the observed flux power spectra, over the full redshift range $2 < z < 3$. Additionally, by deblending the absorption features of Lyman- α spectra into a sum of thermally broadened individual lines, we find superb agreement with the observed lower cutoff of the line-width distribution (Fig. 5) and abundances of neutral hydrogen column densities per unit redshift. This concordance between Lyman- α data and simulation results, which are based on the most recent cosmological parameters, also suggests that the inclusion of blazar heating alleviates previous tensions on constraints of the normalization of the density power spectrum, σ_8 , derived from Lyman- α measurements and other cosmological data.

5 Implications for the formation of dwarf galaxies and galaxy clusters

We have seen that blazar heating dramatically changes the thermal history of the diffuse IGM, which necessarily implies a number of important implications for late-time structure formation (Pfrommer *et al.* 2012). Unlike photoionization models, which typically invoke the heating at reionization, blazar heating provides a well defined, time-dependent entropy enhancement that rises dramatically after $z \sim 2$, suppressing the formation of late forming dwarf galaxies. On small scales, thermal pressure opposes gravitational collapse. This introduces a characteristic length and mass scale below which galaxies do not form. A hotter intergalactic medium implies a higher thermal pressure and a higher Jeans mass M_J at redshift z ,

$$M_J \propto \frac{c_s^3(z)}{\sqrt{G^3 \rho(z)}} \propto \left(\frac{T^3(z)}{G^3 \rho(z)} \right)^{1/2} \rightarrow \frac{M_{J,\text{blazar}}}{M_{J,\text{photo}}} \approx \left(\frac{T_{\text{blazar}}}{T_{\text{photo}}} \right)^{3/2} \gtrsim 30, \quad (2)$$

where c_s , ρ , and T_{IGM} are the sound speed, density, and temperature of the IGM, respectively, and G is Newton's gravitational constant. That is, blazar heating increases M_J by 30 over pure photoheating models.

However, there are complications due to non-linear collapse and a delayed pressure response in an expanding universe. This causes a slight reduction of the suppression factor (Fig. 6). Hence, our redshift-dependent entropy enhancement due to blazar heating increases the characteristic

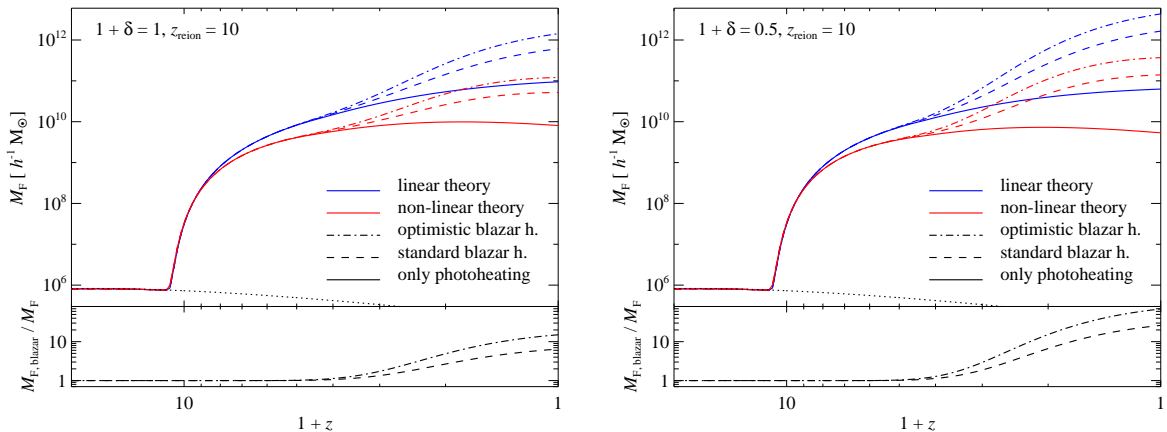


Figure 6: Blazar heating suppresses the formation of late-forming dwarf galaxies. Redshift evolution of the filtering mass, M_F , for the cosmic mean density, $\delta = 0$ (left) and for a void with mean overdensity, $\delta = -0.5$, (right). We contrast M_F in the standard cosmology that employs only photoheating (solid) to the case of blazar heating in our standard model (dashed) and optimistic model (dash-dotted). In the bottom panels, we show the ratio of M_F in our respective blazar heating models to those without blazars. To estimate the effect of nonlinear structure formation on the filtering mass, we compare the linear theory M_F (blue) to the nonlinear theory M_F (red) where we used a correction function derived from hydrodynamic simulations (from Pfrommer *et al.* 2012).

halo mass below which dwarf galaxies cannot form by a factor of approximately 10 (50) at mean density (in voids) over that found in the standard model, preventing the formation of late-forming dwarf galaxies. This may help resolve the “missing satellites problem” in the Milky Way of the low observed abundances of dwarf satellites compared to cold dark matter simulations and may bring the observed early star formation histories into agreement with galaxy formation models. At the same time, it is a very plausible explanation of the “void phenomenon” (Peebles & Nusser 2010) by suppressing the formation of galaxies within existing dwarf halos, thus reconciling the number of dwarfs in low-density regions in simulations and the paucity of those in observations.

Finally, this suggests a scenario for the origin of the cool core/non-cool core bimodality in galaxy clusters and groups, which are separated into different classes depending on their core temperatures. Early forming galaxy groups are unaffected because they can efficiently radiate the additional entropy, developing a cool core. However, late-forming groups do not have sufficient time to cool before the elevated entropy enhancement is gravitationally reprocessed through successive mergers—counteracting cooling and potentially raising the core entropy further to potentially form a non-cool core cluster.

6 Conclusions and Outlook

In a series of papers, we have proposed a novel plasma-astrophysical mechanism that promises transformative and potentially radical changes of our understanding of gamma-ray astrophysics and the physics of the intergalactic medium. This can also alter our picture of the formation of dwarf galaxies and galaxy cluster thermodynamics. Detailed comparisons of predictions of blazar heating with Lyman- α forest data and *Fermi* observation of blazar statistics as well as the isotropic and anisotropy gamma-ray backgrounds have been very successful and encouraging.

Nevertheless, we are clearly only beginning to explore the process and implications of plasma-instability driven blazar heating. Many aspects are only poorly understood and are now starting to be investigated, including the physics of the instability in the regime of non-linear saturation. Detailed cosmological simulations of blazar heating are critical in understanding its impact on non-linear structure formation. We hope that this work motivates fruitful observational and theoretical efforts toward consolidating the presented picture or to modify parts of it.

Acknowledgments

C.P. gratefully acknowledges financial support of the Klaus Tschira Foundation. A.E.B. receives financial support from the Perimeter Institute for Theoretical Physics and the Natural Sciences and Engineering Research Council of Canada through a Discovery Grant. Research at Perimeter Institute is supported by the Government of Canada through Industry Canada and by the Province of Ontario through the Ministry of Research and Innovation. P.C. gratefully acknowledges support from the UWM Research Growth Initiative and from *Fermi* Cycle 5 through NASA grant NNX12AP24G. E.P. acknowledges support by the DFG through Transregio 33.

References

- [1] A. Abdo, *et al.*, *ApJ* **720**, 435 (2010).
- [2] M. Ackermann, *et al.*, 4th Fermi Symposium (2012).
- [3] A. Bret, L. Gremillet, D. Bénisti, *PRE* **81**, 036402 (2010a).
- [4] A. Bret, L. Gremillet, M. E. Dieckmann, *PoP* **17**, 120501 (2010b).
- [5] A.E. Broderick, P. Chang, C. Pfrommer, *ApJ* **752**, 22 (2012).
- [6] A.E. Broderick, C. Pfrommer, E. Puchwein, P. Chang, *subm.* (2013), [arXiv:1308.0340](#).
- [7] P. Chang, A.E. Broderick, C. Pfrommer, *ApJ* **752**, 23 (2012).
- [8] P.F. Hopkins, T. Richards, L. Hernquist, *ApJ* **654**, 731 (2007).
- [9] T.S. Kim, M. Viel, M.G. Haehnelt, R.F. Carswell, S. Cristiani, *MNRAS* **347**, 355 (2004).
- [10] D. Kirkman and D. Tytler, *ApJ* **484**, 672 (1997).
- [11] F. Miniati and A. Elyiv, *ApJ* **770**, 54 (2013).
- [12] A. Neronov and I. Vovk, *Science* **328**, 73 (2010)
- [13] P.J.E. Peebles and A. Nusser, *Nature* **465**, 565 (2010).
- [14] C. Pfrommer, P. Chang, A.E. Broderick, *ApJ* **752**, 24 (2012).
- [15] E. Puchwein, C. Pfrommer, V. Springel, P. Chang, A.E. Broderick, *MNRAS* **423**, 149 (2012).
- [16] R. Schlickeiser, D. Ibscher, M. Supsar, *ApJ* **758**, 102 (2012).
- [17] R. Schlickeiser, S. Krakau, M. Supsar, *ApJ in print* (2013), [arXiv:1308.4594](#).
- [18] T.M. Venters, *ApJ* **710**, 1530 (2010).
- [19] M. Viel, M.G. Haehnelt, V. Springel, *MNRAS* **354**, 684 (2004).